

## Spin-Selective Aharonov-Bohm Oscillations in a Lateral Triple Quantum Dot

F. Delgado,<sup>1,2</sup> Y.-P. Shim,<sup>1</sup> M. Korkusinski,<sup>1</sup> L. Gaudreau,<sup>1,3</sup> S. A. Studenikin,<sup>1</sup> A. S. Sachrajda,<sup>1</sup> and P. Hawrylak<sup>1,2</sup>

<sup>1</sup>*Institute for Microstructural Sciences, National Research Council, Ottawa, Ontario, Canada K1A 0R6*

<sup>2</sup>*Department of Physics, University of Ottawa, Ottawa, Ontario, Canada K1N 6N5*

<sup>3</sup>*Région Québecois sur les Matériaux de Pointe, Université de Sherbrooke, Québec, Canada J1K 2R1*

(Received 19 August 2008; published 26 November 2008)

We present a theory of spin-selective Aharonov-Bohm oscillations in a lateral triple quantum dot. We show that to understand the Aharonov-Bohm (AB) effect in an interacting electron system within a triple quantum dot molecule (TQD) where the dots lie in a ring configuration requires one to not only consider electron charge but also spin. Using a Hubbard model supported by microscopic calculations we show that, by localizing a single electron spin in one of the dots, the current through the TQD molecule depends not only on the flux but also on the relative orientation of the spin of the incoming and localized electrons. AB oscillations are predicted only for the spin singlet electron complex resulting in a magnetic field tunable “spin valve.”

DOI: 10.1103/PhysRevLett.101.226810

PACS numbers: 73.21.La, 73.23.Hk

The Aharonov-Bohm [1] (AB) effect results from the accumulation of phase by a charged particle moving in a ring threaded by a magnetic flux [2,3]. AB oscillations are detected, e.g., in the magnetization of a macroscopic number of electrons in metallic rings [4] as well as in the optical emission from a charged exciton in a nanosize semiconductor quantum ring [5]. At the same time, the preparation, manipulation and detection of individual spins of localized electrons in nanoscale semiconductor systems are important elements of nanospintronic applications [6–8], with efficient generation and detection of spin polarized carriers playing a crucial role. The electron spins can be localized in single and coupled semiconductor quantum dots (QDs) defined and controlled electrostatically [9–14] with potential applications as elements of electron-spin based circuits [15,16], coded qubits [17], entanglers [18], rectifiers and ratchets [19,20]. The spin blockade technique in a double dot system used for the conversion of spin to charge information has played an important role in the development of such applications [21].

We discuss here the possibility of the coexistence of spin blockade with AB oscillations in a lateral TQD in a ring geometry [13,22]. We describe a TQD, shown schematically in Fig. 1(a), where two dots, 1 and 3, are connected to the leads and in addition to dot number 2. A single electron spin is localized in dot 2 by lowering the confining potential. The transport of an additional electron through the TQD will now depend on the relative orientation of the spin of the incoming and localized electrons. If the two spins are antiparallel, as shown in Fig. 1(b), the additional electron can tunnel from the left lead to dot 1, and proceed either directly or through dot 2 to dot 3 and thus to the right lead. In the presence of the magnetic field the two paths acquire a different phase and can interfere, resulting in the AB oscillations of the current amplitude (upper inset). When the spin of the incoming electron is parallel to the

spin of the electron in dot 2, the Pauli exclusion principle prevents tunneling through dot 2, resulting in a single tunneling path and the absence of AB oscillations (lower inset). We present here a theory of the signature of these spin-selective AB oscillations in transport through a TQD. The electronic properties of a TQD are treated by a fully microscopic LCHO-CI approach [23] and by Hubbard and  $t$ - $J$  models with exact many-electron eigenstates obtained using configuration-interaction (CI) method [24]. The Fermi Golden Rule and the sequential tunneling approach [25] are used to calculate the current through the TQD weakly connected to two noninteracting leads. The current

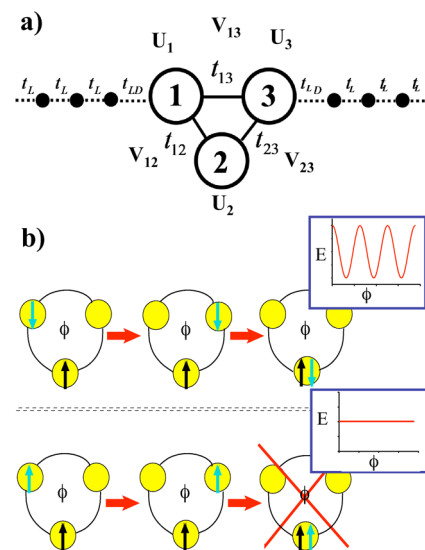


FIG. 1 (color online). (a) Schematic diagram of the TQD close to the QP. (b) Path of an added electron with antiparallel spin can form a loop and the corresponding energy level  $E$  exhibits AB oscillations with the magnetic flux  $\phi$  while path of an electron with parallel spin is spin blocked.

flows when the chemical potential of the TQD is equal to the chemical potential of the leads. This can also be understood in terms of degeneracies of many-electron charge configurations  $(N_1, N_2, N_3)$  with  $N_i$  the number of electrons in dot  $i$ . The degeneracy point described here, referred to as the quadrupole point (QP), involves the one electron configuration  $(0, 1, 0)$  and two-electron configurations  $(1, 1, 0)$ ,  $(0, 2, 0)$ , and  $(0, 1, 1)$ , with one electron always confined in dot 2, as shown in Fig. 1(b).

For clarity we only present results of the Hubbard model with one orbital per dot [22,24]. The Hamiltonian of the TQD subject to a uniform perpendicular magnetic field,  $\mathbf{B} = B\hat{z}$ , is given by

$$H = \sum_{i,\sigma} E_{i\sigma} d_{i\sigma}^\dagger d_{i\sigma} + \sum_{\sigma,i,j;i \neq j} \tilde{t}_{ij} d_{i\sigma}^\dagger d_{j\sigma} + \sum_i U_i n_{i\uparrow} n_{i\downarrow} + \frac{1}{2} \sum_{i,j;i \neq j} V_{ij} \varrho_i \varrho_j, \quad (1)$$

where the operators  $d_{i\sigma}$  ( $d_{i\sigma}^\dagger$ ) annihilate (create) an electron with spin  $\sigma = \pm 1/2$  on orbital  $i$  ( $i = 1, 2, 3$ ).  $n_{i\sigma} = d_{i\sigma}^\dagger d_{i\sigma}$  and  $\varrho_i = n_{i\uparrow} + n_{i\downarrow}$  are the spin and charge density on orbital  $i$ . Each dot is represented by a single orbital with energy  $E_{i\sigma} = E_i + g^* \mu_B B \sigma + E_0$ , where  $g^*$  is the effective Landé  $g$  factor,  $\mu_B$  is the Bohr magneton and  $E_0$  is the energy shift measured from the Fermi level of the leads and tunable by external gates. The dots are connected by magnetic field dependent hopping matrix elements  $\tilde{t}_{ij} = t_{ij} e^{2\pi i \phi_{ij}}$  [22]. For the three dots in an equilateral configuration  $\phi_{12} = \phi_{23} = \phi_{31} = -\phi/3$  and  $\phi_{ji} = -\phi_{ij}$ , where  $\phi = BA/\phi_0$  is the number of flux quanta threading the area  $A$  of the triangle,  $\phi_0 = hc/e$ ,  $e$  is the electron charge,  $c$  is the speed of light and  $\hbar$  is the Planck's constant. The interacting part of the Hamiltonian is parametrized by the on-site Coulomb repulsion,  $U_i$ , and the interdot direct repulsion term  $V_{ij}$ .

In order to describe transport through the TQD we first determine the QP of the isolated TQD. We start by determining the ‘‘classical QP’’ where we neglect the interdot tunneling and require the four configurations  $A \equiv (1, 1, 0)$ ,  $B \equiv (0, 2, 0)$ ,  $C \equiv (0, 1, 1)$  and  $D \equiv (0, 1, 0)$  to have equal energy. Their energies are  $\epsilon_A = E_1 + E_2 + V_{12} + 2E_0$ ,  $\epsilon_B = 2E_2 + U_2 + 2E_0$ ,  $\epsilon_C = E_2 + E_3 + V_{23} + 2E_0$ , and  $\epsilon_D = E_2 + E_0$ . The QP condition without tunneling requires  $\epsilon_A = \epsilon_B = \epsilon_C = \epsilon_D + \mu_L$ , where  $\mu_L$  is the chemical potential of the leads. This implies that at the QP  $E_1^Q = \mu_L - E_0 - V_{12}$ ,  $E_2^Q = \mu_L - E_0 - U_2$  and  $E_3^Q = \mu_L - E_0 - V_{23}$ .

Let us consider now the case of finite tunneling matrix elements. The  $(0, 1, 0)$  charge configuration describes the two spin states of an electron localized in dot 2,  $|2\sigma\rangle \equiv d_{2\sigma}^\dagger |0\rangle$  with energy  $E_2$  ( $|0\rangle$  is the vacuum state). The two-electron classical charge configurations  $(1, 1, 0)$ ,  $(0, 2, 0)$ , and  $(0, 1, 1)$  correspond to the following quantum spin singlet configurations:  $|S_1\rangle = \frac{1}{\sqrt{2}}(d_{1\uparrow}^\dagger d_{2\downarrow}^\dagger + d_{2\uparrow}^\dagger d_{1\downarrow}^\dagger)|0\rangle$ ,

$|S_2\rangle = d_{2\uparrow}^\dagger d_{2\downarrow}^\dagger |0\rangle$ , and  $|S_3\rangle = \frac{1}{\sqrt{2}}(d_{2\uparrow}^\dagger d_{3\downarrow}^\dagger + d_{3\uparrow}^\dagger d_{2\downarrow}^\dagger)|0\rangle$ . The Hamiltonian describing the motion of the spin singlet pair takes the form

$$\hat{H}_S = \begin{pmatrix} \epsilon_A & \sqrt{2}t_{12}e^{-2\pi i\phi/3} & t_{13}e^{2\pi i\phi/3} \\ \sqrt{2}t_{12}e^{2\pi i\phi/3} & \epsilon_B & \sqrt{2}t_{23}e^{-2\pi i\phi/3} \\ t_{13}e^{-2\pi i\phi/3} & \sqrt{2}t_{23}e^{2\pi i\phi/3} & \epsilon_C \end{pmatrix}.$$

At the classical QP, we have  $\epsilon_A = \epsilon_B = \epsilon_C$ . If  $t_{23} = t_{12} = t_{13}/\sqrt{2}$ , we can diagonalize the Hamiltonian exactly by Fourier transforming into a new basis:  $|K_1\rangle = 1/\sqrt{3}(|1\rangle + |2\rangle + |3\rangle)$ ,  $|K_2\rangle = 1/\sqrt{3}(|1\rangle + e^{i2\pi/3}|2\rangle + e^{i4\pi/3}|3\rangle)$ , and  $|K_3\rangle = 1/\sqrt{3}(|1\rangle + e^{-i2\pi/3}|2\rangle + e^{-i4\pi/3}|3\rangle)$  with eigenvalues  $\epsilon_1 = E - 2|t| \cos(2\pi\phi/3)$ ,  $\epsilon_2 = E - 2|t| \cos[2\pi(\phi + 1)/3]$ , and  $\epsilon_3 = E - 2|t| \cos[2\pi(\phi - 1)/3]$ , and  $t \equiv t_{13}$ . Since one of the electrons is kept in dot 2, the energy spectrum of a pair of singlet electrons is essentially the same as that of a single electron added to a resonant TQD, with the energy levels oscillating with a period of one flux quantum [22]. Away from the resonance the level crossing is replaced by anticrossing.

A pair of spin triplet electrons describes only  $(1, 1, 0)$  and  $(0, 1, 1)$  charge configurations. The corresponding two spin triplet configurations for  $S_Z = 1$  are  $|T_1\rangle = d_{1\uparrow}^\dagger d_{2\uparrow}^\dagger |0\rangle$  with energy  $\epsilon_A(B)$  and  $|T_2\rangle = d_{2\uparrow}^\dagger d_{3\uparrow}^\dagger |0\rangle$  with energy  $\epsilon_C(B)$ , with  $\epsilon_A(B) = \epsilon_A + g^* \mu_B B S_Z$ . The eigenenergies of the  $2 \times 2$  triplet Hamiltonian are  $\epsilon_{\bar{T}}^\pm = 1/2\{\epsilon_A(B) + \epsilon_C(B) \pm [(\epsilon_A(B) - \epsilon_C(B))^2 + 4|t_{13}|^2]^{1/2}\}$ . By comparing the singlet and triplet eigenvalues we see that singlet is the ground state at  $B = 0$  and the eigenvalues of the triplet do not oscillate as a function of the magnetic field. Even at this qualitative level, we obtain a remarkable result that triplet states do not oscillate with the magnetic field while singlets do.

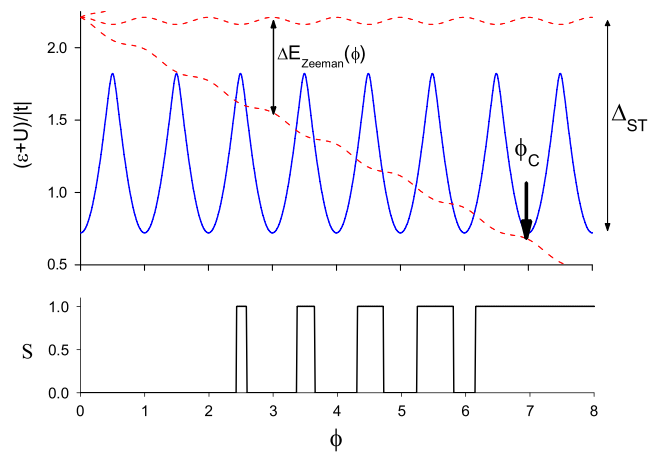


FIG. 2 (color online). Low energy spectrum of the two-electron TQD (upper panel) and total spin of the ground state (lower panel) at the QP versus the magnetic flux. The QP condition was found numerically for  $\delta_1 = \delta_3 = 2.44|t|$  and  $\delta_2 = 2.77|t|$ .

In the case of finite tunneling each classical configuration is no longer an eigenstate of the system. Therefore, we will define QP as the point in the parameter space where the ground state energies of two and one electrons differ by  $\mu_L$  and the three degenerate two-electron configurations are found with the same probabilities. Then, at the QP  $E_i = E_i^0 + \delta_i$ , where the energies  $\delta_i$  are quantum corrections that are obtained numerically, with  $\delta_1 = \delta_3$  for the symmetric case described here.

We shall analyze now the magnetic field dependence of the two-electron energy spectrum close to the QP. The numerical CI calculations include the full Hilbert space generated from the three orbital levels. Hubbard parameters were obtained from the LCHO calculation with an interdot distance of 61.2 nm:  $t = -0.23$  meV,  $U_i = 50|t|$  and  $V_{ij} = 10|t|$ , and  $g^* = -0.44$  of GaAs is used. The parameters are similar to the ones obtained from first experiment in Ref. [24] except for the larger tunneling matrix element and smaller TQD area. The upper panel of Fig. 2 shows the lower part of the energy spectrum for  $E_0 = -|t|$ , while the lowest panel indicates the total spin of the ground state. We find the ground state at  $B = 0$  to be spin singlet (solid line) with the triplet an excited state with energy  $\Delta_{ST}$  above the singlet. The singlet energy oscillates with  $B$  with period of one flux quantum while the energy of the triplet decreases monotonically with increasing magnetic field due to Zeeman energy. Notice that energy of the triplet shows a small oscillation due to a coupling with higher energy configurations. The oscillating singlet energy and monotonically decreasing triplet energy leads to a number of transitions between singlet and triplet with increasing magnetic field. These transitions interrupt the AB oscillations of the singlet, and lead to their end at a critical value of the magnetic field,  $B_C = \Delta_{ST}/g^* \mu_B$ , with corresponding critical flux  $\phi_C = AB_C/\phi_0$ , indicated in Fig. 2. With  $\Delta_{ST}$  of the order of  $\approx 0.2$  meV and Zeeman energy 0.02 meV/T [8] the expected values of  $B_C$  are  $\approx 1$ –10 T. Above  $B_C$  the triplet is the ground state. Hence the presence of a trapped electron should lead to AB oscillations of the tunneling electron, interrupted and eventually terminated by the singlet-triplet transitions.

Figure 3 shows the dominant charge ground state configurations of the TQD at two different values of the magnetic flux quantum,  $\phi = 0$  (upper panel) and  $\phi = 0.44$  (lower panel), versus the voltages  $V_{g1}$  and  $V_{g2}$  for a given  $E_0 = -|t|$ . The on-site energies  $E_i$ 's were assumed to change linearly with the voltages  $V_{g1}$  and  $V_{g2}$ ,  $E_i = \alpha_i V_{g1} + \beta_i V_{g2} + \gamma_i$ , with  $\alpha_i, \beta_i$  extracted from experiment in Ref. [13]. We see that for  $\phi = 0$  the stability diagram shows only a triple point, while for  $\phi = 0.44$  the QP is clearly visible.

We now discuss how these spin-selective AB oscillations can be observed in transport. Following Ref. [26], the Hamiltonian of the TQD connected to two leads is given by  $H = H_L + H_{TQD} + H_{LD}$ , where  $H_L$  is the Hamiltonian of the two noninteracting leads.  $H_{TQD}$  corresponds to the

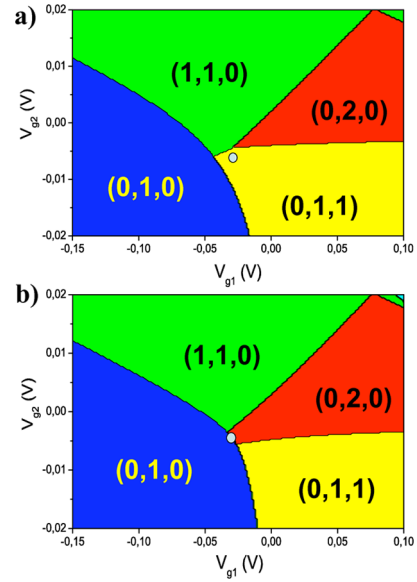


FIG. 3 (color online). Stability diagram as a function of  $V_{g1}$  and  $V_{g2}$  of the TQD close to the QP with charge configurations  $(1, 1, 0)$ ,  $(0, 2, 0)$ ,  $(0, 1, 1)$  and  $(0, 1, 0)$  at (a)  $\phi = 0$  and (b),  $\phi = 0.44$ . The classical QP ( $t = 0$ ) is found at  $V_{g1} = V_{g2} = 0$  while the quantum one at  $\phi = 0.44$  is indicated by the white circle.

isolated triple dot with the on-site energies changed by the applied bias  $\Delta V$  as  $E_{i\sigma} \rightarrow E_{i\sigma} - \Delta V/2$ .  $H_{LD}$  is the tunneling Hamiltonian between the leads and the TQD. The leads are described with a one-dimensional tight-binding model with nearest neighbor hopping  $t_L$ , on-site energies  $\epsilon_L$  ( $\epsilon_R$ ) for the left (right) leads, and dots and leads hopping  $t_{LD}$  [26]. The current through the system is evaluated using a set of master equations for the occupation probabilities within the sequential tunneling approximation [25]. This approach neglects higher order processes such as cotunneling, important for high tunnel-coupling strengths and for temperatures below the Kondo temperature [27–29]. The occupation probabilities are then calculated using a detailed balance condition imposed by the conservation of charge. The spin components of the current in the linear regime in the lowest order in the coupling  $t_{LD}$  and at zero temperature are then given by  $I^\sigma = e\pi/(2\hbar)|t_{LD}|^2\rho(\epsilon_F)\Delta VC^\sigma\delta(\epsilon_F - (\epsilon_{2,G} - \epsilon_{1,G}))$  where  $\epsilon_{2,G}(\epsilon_{1,G})$  is the ground state energy of the two (one) electrons in a TQD and  $\rho(\epsilon_F)$  is the density of states in the leads at the Fermi level, with  $\rho_L(\epsilon_{F,L}) \approx \rho_R(\epsilon_{F,R})$ .  $C^\sigma = 1/3$  for  $\sigma = \downarrow$  (singlet ground state) and  $C^\sigma = 1$  for  $\sigma = \uparrow$  (triplet ground state). Note that the probability of having the extra electron in each dot at the QP is exactly 1/3 for the singlet ground state while for the triplet the extra electron can be found in dots 1 and 3 with probability 1/2.

Next we present the linear conductance  $G = I/\Delta V$ . The calculations were done at 50 mK ( $k_B T = 0.0145|t|$ ),  $\Delta V = 2 \times 10^{-3}|t|$  and  $\mu_L = 0$ . In addition,  $|t_L| = 23.72$  meV  $\gg |t|$ ,  $E_0, \Delta V$ . Since transport through the

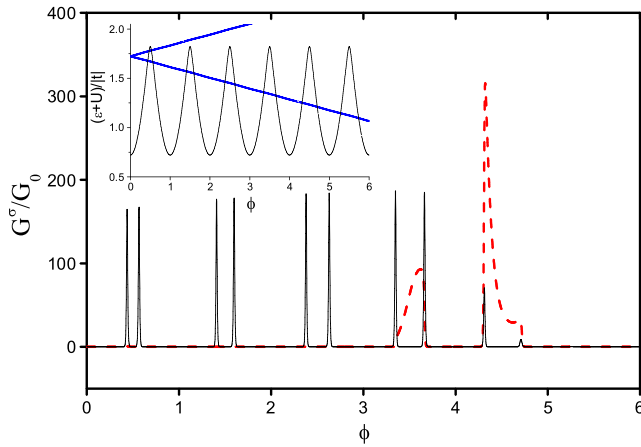


FIG. 4 (color online). Spin-down (solid line) and spin-up (dashed line) components of the conductance in units of  $G_0 = e^2|t_{LD}|^2/\hbar|t_L|^2$  versus the number of flux quantum  $\phi$  for the same parameters as in Fig. 2. The inset shows the energy spectrum of the two-electron complex (as in Fig. 2), together with the one electron lowest levels (thick blue line).

TQD is allowed whenever the single-particle and the two-particle ground states are on resonance, the AB oscillations of the energy spectra lead to repeated peaks in the current. The spin components of the conductance  $G^\sigma = I^\sigma/\Delta V$  are shown in Fig. 4. At low magnetic fields, the spin-down current is dominant and transport is mainly through the lowest oscillating singlet state. When the ground state of two particles becomes triplet, spin up current is dominant until the current is totally suppressed. The results are valid for temperature higher than the Kondo temperature, which can be made exponentially small by reducing the coupling of a TQD to the leads.

In summary, we presented a theory of spin-selective AB oscillations in a ringlike TQD with one electron localized in one dot. We showed that only the energy of the singlet oscillates as a result of the interference between the two possible paths. The magnetic field polarizes the spin of the localized electron leading to the transport of electrons with a specific spin polarization. The AB oscillation of the singlet electron pair is reflected as periodic peaks in the spin-down polarized current. At higher magnetic field, the Zeeman energy causes a singlet-triplet transition, which results in a change of the dominant spin component of the current.

The authors acknowledge support by the QuantumWorks Network and the Canadian Institute for Advanced Research.

- [1] Y. Aharonov and D. Bohm, Phys. Rev. **115**, 485 (1959).  
 [2] M. Büttiker, Y. Imry, and M. Y. Azbel, Phys. Rev. A **30**, 1982 (1984).  
 [3] R. A. Webb, S. Washburn, C. P. Umbach, and R. B. Laibowitz, Phys. Rev. Lett. **54**, 2696 (1985).

- [4] L. P. Lévy, G. Dolan, J. Dunsmuir, and H. Bouchiat, Phys. Rev. Lett. **64**, 2074 (1990).  
 [5] M. Bayer, M. Korkusinski, P. Hawrylak, T. Gutbrod, M. Michel, and A. Forchel, Phys. Rev. Lett. **90**, 186801 (2003).  
 [6] *Semiconductor Spintronics and Quantum Computation*, edited by D. D. Awschalom, D. Loss, and N. Samarth, Series on Nanoscience and Technology, Vol. XVI (Springer, New York, 2002).  
 [7] I. Žutić, J. Fabian, and S. Das Sarma, Rev. Mod. Phys. **76**, 323 (2004).  
 [8] A. S. Sachrajda, P. Hawrylak, and M. Ciorga, in *Electronic Transport in Quantum Dots*, edited by J. P. Bird (Kluwer Academic, Boston, 2003).  
 [9] M. Ciorga, A. S. Sachrajda, P. Hawrylak, C. Gould, P. Zawadzki, S. Jullian, Y. Feng, and Z. Wasilewski, Phys. Rev. B **61**, R16315 (2000).  
 [10] F. H. L. Koppens, C. Buizert, K. J. Tielrooij, I. T. Vink, K. C. Nowack, T. Meunier, L. P. Kouwenhoven, and L. M. K. Vandersypen, Nature (London) **442**, 766 (2006).  
 [11] J. R. Petta, A. C. Johnson, J. M. Taylor, E. A. Laird, A. Jacoby, M. D. Lukin, C. M. Marcus, M. P. Hanson, and A. C. Gossard, Science **309**, 2180 (2005).  
 [12] A. Vidan, R. M. Westervelt, M. Stopa, M. Hanson, and A. C. Gossard, J. Supercond. **18**, 223 (2005).  
 [13] L. Gaudreau, S. Studenikin, A. Sachrajda, P. Zawadzki, A. Kam, J. Lapointe, M. Korkusinski, and P. Hawrylak, Phys. Rev. Lett. **97**, 036807 (2006).  
 [14] T. Ihn, M. Sigrist, K. Ensslin, W. Wegscheider, and M. Reinwald, New J. Phys. **9**, 111 (2007).  
 [15] J. A. Brum and P. Hawrylak, Superlattices Microstruct. **22**, 431 (1997).  
 [16] D. Loss and D. P. DiVincenzo, Phys. Rev. A **57**, 120 (1998).  
 [17] P. Hawrylak and M. Korkusinski, Solid State Commun. **136**, 508 (2005).  
 [18] D. S. Saraga and D. Loss, Phys. Rev. Lett. **90**, 166803 (2003).  
 [19] M. Stopa, Phys. Rev. Lett. **88**, 146802 (2002).  
 [20] A. Vidan, R. M. Westervelt, M. Stopa, M. Hanson, and A. C. Gossard, Appl. Phys. Lett. **85**, 3602 (2004).  
 [21] K. Ono, D. G. Austing, Y. Tokura, and S. Tarucha, Science **297**, 1313 (2002).  
 [22] F. Delgado, Y.-P. Shim, M. Korkusinski, and P. Hawrylak, Phys. Rev. B **76**, 115332 (2007).  
 [23] I. Puerto Gimenez, M. Korkusinski, and P. Hawrylak, Phys. Rev. B **76**, 075336 (2007).  
 [24] M. Korkusinski, I. Puerto Gimenez, P. Hawrylak, L. Gaudreau, S. A. Studenikin, and A. S. Sachrajda, Phys. Rev. B **75**, 115301 (2007).  
 [25] B. Muralidharan and S. Datta, Phys. Rev. B **76**, 035432 (2007).  
 [26] F. Delgado and P. Hawrylak, J. Phys. Condens. Matter **20**, 315207 (2008).  
 [27] K. Ingersent, A. W. W. Ludwig, and I. Affleck, Phys. Rev. Lett. **95**, 257204 (2005).  
 [28] T. Kuzmenko, K. Kikoin, and Y. Avishai, Phys. Rev. Lett. **96**, 046601 (2006).  
 [29] R. Žitko and J. Bonča, Phys. Rev. B **77**, 245112 (2008).